X-Band FMCW Radar System with Variable Chirp Duration

Christoph Schroeder
Department of Telecommunications
Hamburg University of Technology
Hamburg, Germany
Email: christoph.schroeder@tu-harburg.de

Hermann Rohling
Department of Telecommunications
Hamburg University of Technology
Hamburg, Germany
Email: rohling@tu-harburg.de

***Abstract*— For application in a short range ground based surveillance radar a combination between frequency modulated continuous wave (FMCW) transmit signals and a receive antenna array system is considered in this paper. The target echo signal is directly down converted by the instantaneous transmit frequency.**

The target range R will be estimated based on the measured frequency shift f_B between transmit and receive signal. Due to an extremely short chirp duration T_{chirp}, the target radial velocity v_r has only a very small influence to the measured frequency shift f_B. Therefore the radial velocity v_r will not be measured inside a single FMCW chirp but in a sequence of chirp signals and inside each individual range gate. Finally, the target azimuth angle is calculated utilizing the receive antenna array and applying a digital beamforming scheme.

Furthermore, in order to unambiguously measure even high radial velocities, a variable chirp duration is proposed on a dwell to dwell basis.

I. Introduction

In this paper an FMCW transmit signal with extremely short chirp duration T_{chirp} is proposed for a ground based surveillance radar. Due to the short chirp duration the measured frequency shift f_B is always positive. Therefore, a single receive channel (I-channel) will be implemented and is sufficient in the radar receiver. The additional Q-channel can be avoided in this case which reduces the computation complexity and removes the need for precise synchronization between I- and Q-channel. Fig. 1 depicts an application example, where the proposed ground based surveillance radar system is used to monitor a marine bay. Based on the short chirp duration and the rapid chirp repetition the Doppler frequencies f_D in the echo signals have only a small interfering influence onto the range measurement accuracy. All target ranges will show a positive frequency difference f_B between transmit and receive signal, which makes a single receive channel technique in the hardware design feasible. The main contribution to the frequency difference f_B is based on the target range R and only a negligible influence from the Doppler frequency f_D can be observed in the range measurement procedure in a single target and even in a multiple target situation.

But due to the specific system parameters the measured Doppler frequencies can be ambiguous in some cases. Therefore, a low computation complexity technique for resolving Doppler frequency ambiguities even in multiple target situations is considered in this paper.

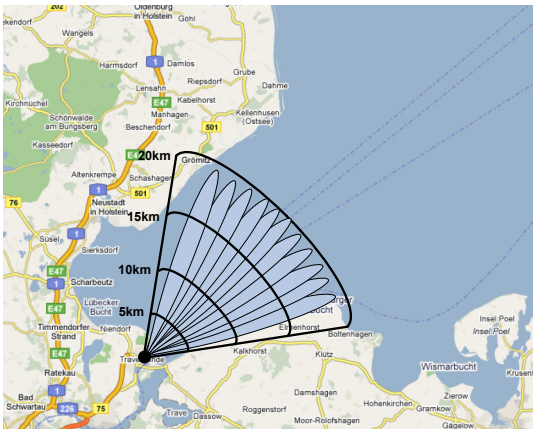

Fig. 1. Multiple receive beams

The paper is organized as follows: Section II gives an overview of the system design, in Section III the signal processing procedure is discussed and analyzed. In Section IV simulation results of the designed radar system are presented.

II. System Overview

A surveillance radar system with a high target detection probability inside a large detection range is considered in this paper. A simultaneous measurement of target range R, radial velocity v_r and azimuth angle φ is required even in multiple target situations.

A. Antenna Concept

Fig. 2 shows the system design and the array antenna concept in a block diagram. In total, one transmit and M parallel receive (Rx) antennas are utilized. The receive antennas are positioned in a uniform linear array (ULA) allow the direct application of digital beamforming for target detection.

After receiving the target echo signal, it is being amplified, filtered and demodulated. The down converted echo signal will be sampled and three different FFT are processed to measure target range, radial velocity and azimuth angle simultaneously. Due to the high coherent processing gain, target detection is possible even in weak target and very low signal to noise ratio (SNR) situations.

978-1-4244-5812-7/10/$26.00 ©2010 IEEE

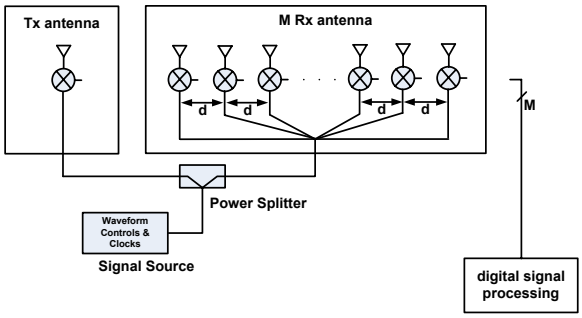

Fig. 2. Antenna array consisting of the transmit and receive antenna block

B. Waveform Design

The radar waveform is a classical FMCW signal, which is depicted in Fig. 3. But the chirp duration is extremely short in this waveform. An FMCW radar emits a continuous wave signal with a linear frequency modulation from f_0 up to $f_0 + f_{\text{sweep}}$ inside a chirp duration T_{chirp}. The system parameter f_{sweep} describes the radar signal bandwidth. The transmit waveform $u(t)$ has a constant envelope and can analytically be denoted as

$$u(t) = A_{\text{Tx}} \cos\left(\theta_{\text{Tx}}(t)\right) \tag{1}$$

where A_{Tx} is the signal amplitude and $\theta_{\text{Tx}}(t)$ the instantaneous transmit signal phase calculated as

$$\theta_{\text{Tx}}(t) = 2\pi \int_0^t f(x)dx = 2\pi \left[f_0 t + \frac{f_{\text{sweep}}}{2T_{\text{chirp}}} t^2 \right] \tag{2}$$

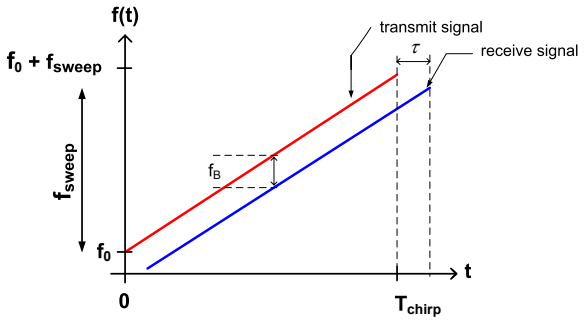

Fig. 3. Transmit and receive signal for a single chirp

The received target echo signal $r(t)$ is a reflected, attenuated and time delayed copy of the transmit signal $u(t)$ which can be described by

$$r(t) = A_{\text{Rx}}\, u(t-\tau) = A_{\text{Tx}}\, A_{\text{Rx}} \cos\left(\theta_{\text{Rx}}(t)\right) \tag{3}$$

where the signal phase $\theta_{\text{Rx}}(t)$ can be described by

$$\theta_{\text{Rx}}(t) = 2\pi \left[f_0(t-\tau) + \frac{f_{\text{sweep}}}{2T_{\text{chirp}}}(t-\tau)^2 \right] \tag{4}$$

In the following analysis the amplitudes A_{Tx} of the transmit and A_{Rx} of the receive signal are normalized to $A_{\text{Tx}} = A_{\text{Rx}} = 1$. The received signal is down converted with the instantaneous transmit signal and after low-pass filtering the base band signal $s(t)$ can be obtained.

In case of a moving target with constant radial velocity v_r the target range $R(t)$ is linearly time dependent according to the assumed linear movement $R(t) = R_0 + v_r t$. The time delay $\tau(t)$ is also time dependent and can be described by

$$\tau(t) = 2\,\frac{R_0 + v_r t}{c} \tag{5}$$

With these remarks the base band signal $s(t)$ in the receiver can be described as follows:

$$s(t) = \cos\left(\theta_d(t)\right) \tag{6}$$

where the phase θ_d of the down converted receive signal $s(t)$ for targets with constant redial velocities can be described by

$$\theta_d(t) = 2\pi \left(2\frac{R_0}{\lambda} + 2\frac{v_r}{\lambda} t + 2\frac{f_{\text{sweep}}}{T_{\text{chirp}}} \frac{R_0}{c} t \right) \tag{7}$$

The frequency difference between transmit and target echo signal, the so-called beat frequency f_B, is influenced by the target range R_0 and the radial velocity v_r and can analytically be described as follows:

$$\begin{aligned} f_B &= \frac{1}{2\,\pi} \frac{\mathrm{d}}{\mathrm{dt}} \theta_d(t) \\ &= 2\frac{v_r}{\lambda} + 2\frac{f_{\text{sweep}}}{T_{\text{chirp}}} \frac{R_0}{c} = f_R - f_D \end{aligned} \tag{8}$$

with the Doppler frequency f_D defined as

$$f_D = -\frac{2v_r}{\lambda} \tag{9}$$

Due to the specific system design parameters and the short chirp duration the Doppler frequency f_D has only a very small influence to the range measurement characterized by f_R during a single chirp.

The baseband signal $s(k)$ can therefore be simplified to

$$s(k) = \cos\left(2\pi\left(\varphi_0 + f_R k T_{\text{sample}}\right)\right) \tag{10}$$

where $f_R = 2\frac{R_0}{c}\frac{f_{\text{sweep}}}{T_{\text{chirp}}}$ is the target range dependent frequency shift, $\varphi_0 = \frac{2R_0}{\lambda}$ is the initial phase, T_{sample} is the sampling time and $k \in [0, K-1]$ is the sample index.

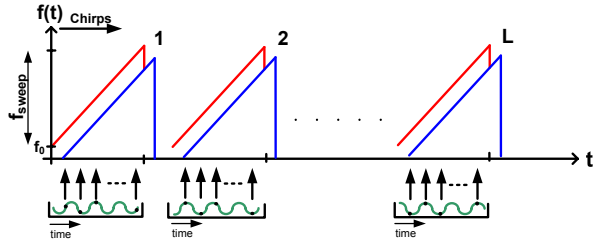

Fig. 4. Frequency of the received and transmitted signal during L chirp signals

The next step is to consider the receive signal during L consecutive chirp signals of duration T_{chirp} each. The corresponding transmit and receive signals are depicted in Fig. 4.

According to previous calculations, the time-discrete baseband signal can be described by

$$s(k,l) = \cos\left(2\pi\left(\varphi_0 + f_R k T_{\text{sample}} - f_D l T_{\text{chirp}}\right)\right) \tag{11}$$

where $f_D = -\frac{2v_r}{\lambda}$ is the Doppler frequency and $l \in [0, L-1]$ is the chirp index.

The final step of the radar echo signal analysis is the addition of the antenna array to the system. Fig. 2 shows a block diagram of the proposed FMCW receive antenna network with M parallel receive (Rx) channels. Due to the azimuth position of the target, a linear phase shift can be observed in the receive signal between consecutive antennas. These phase shift can be exploited in order to obtain the corresponding frequency and hence the direction of arrival (DOA).

According to previous calculations, the time-discrete baseband signal can be described by

$$s(k,l,m) = \cos\left(2\pi\left(\varphi_0 + f_R\, k\, T_{\text{sample}} - f_D\, l\, T_{\text{chirp}} + f_A\, m\right)\right) \quad (12)$$

where $f_A = \frac{d}{\lambda}\sin(\varphi)$ is the spatial frequency introduced from antenna to antenna and $m \in [0, M-1]$ is the antenna index.

Eq. 12 consists of a constant phase offset φ_0 (first term), range dependent frequency shift f_R (second term) and velocity dependent frequency shift f_D (third term) and the azimuth angle dependent frequency contribution f_A (forth term). The additional phase contribution $\varphi_A = 2\pi f_A\, m$ can be considered as a linear phase shift between adjacent antennas.

III. Signal Processing

The signal processing procedure can be divided into three different parts. First of all, the target range R will be measured inside each single chirp signal. The received signal sequence $s(k)$ is therefore transformed by an FFT into the frequency domain $S(u)$ and the beat frequency f_B and the resulting target range R will be measured. Secondly, the target radial velocity v_r is estimated by an FFT inside each single range gate u and over a sequence of L adjacent chirp signals $S_l(u)$, resulting into $S(u,v)$. Finally, the target azimuth angle φ is calculated based again on an FFT applied inside each range-Doppler cell $(\hat{u},\hat{v})$ and based on all M receive antenna signals $S_m(u,v)$.

The three dimensional FFT processing of the acquired bandpass signal $s(k)$ results in the three dimensional spectrum $S(u,v,w)$. The calculated spectrum $S(u,v,w)$ will be analyzed in the target detection process and the maximum peak amplitude $(\hat{u},\hat{v},\hat{w})$ determines the target parameters. It describes the detected target and the estimation for target range R, radial velocity v_r and azimuth angle φ can be carried out.

In the case of an FFT with K sampling values inside a single chirp duration T_{chirp}, the range resolution can be calculated as $\Delta R = \frac{c}{2f_{\text{sweep}}}$, where f_{sweep} is the signal bandwidth. The maximum unambiguous target range corresponds to the maximum detectable beat frequency f_B. Thus, it can be derived to $R_{\max} = \Delta R\frac{K}{2}$.

The radial velocity v_r and the related Doppler frequency f_D measurement is unambiguous only inside an interval from 0 to $f_{D,\max} = \frac{1}{T_{\text{chirp}}}$. The radial velocity resolution can be derived from the Doppler frequency resolution to be $\Delta v_r = 2\frac{v_{\max}}{L}$.

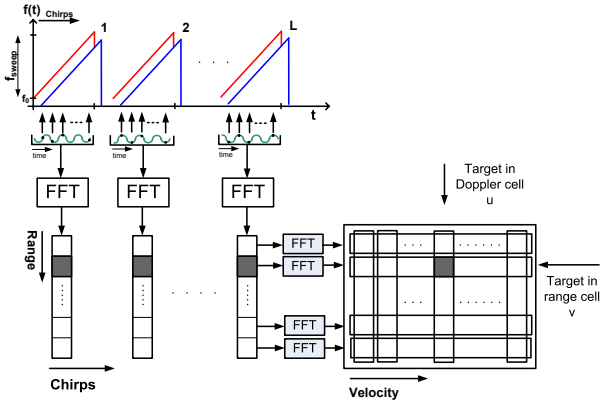

Fig. 5. Range and Doppler processing of consecutive chirps

Due to the distance of $d = \frac{\lambda}{2}$ between two adjacent antenna elements and according to the spatial sampling theorem, azimuth angles in the range of $\varphi \in [-\frac{\pi}{2}, \frac{\pi}{2}]$ can be measured an unambiguous way. The resolution in azimuth direction depends on the 3dB beamwidth of the receive beam.

IV. Doppler Frequency Ambiguity Resolution

In this section a low computation complexity algorithm is discussed to extend the unambiguous Doppler frequency measurement interval.

As stated before, an unambiguous Doppler frequency measurement is only possible in the range of $f_D \in [-1/(2T_{\text{chirp}}), 1/(2T_{\text{chirp}})]$, i.e. up to half of the chirp repetition frequency (CRF). The achievable range does not meet the system requirements for the ground based surveillance radar investigated.

The applied algorithm is based on the Chinese remainder theorem (CRT), but is not only valid for integer-valued measurements, but also for real-valued input data[1]. Additionally, ambiguity resolution and detection are combined leading to a much better detection performance in terms of SNR for a given probability of detection and false alarm.

A. Variable Chirp Duration

A transmit signal block consists of L adjacent FMCW chirp signals with constant chirp duration T_{chirp}. Assume 2 or 3 adjacent transmit signal blocks with different chirp durations $T_{\text{chirp},n}$, $n = [1,2,3]$ have been transmitted. In this case the length of the unambiguous interval on the v_r axis varies. Hence the chirp repetition frequency (CRF), which also is twice the maximum Doppler frequency $f_{D_{\max}}$, will change accordingly leading to an altered length of the unambiguous Doppler frequencies f_D interval. Any Doppler frequency f_D larger than the maximum Doppler frequency $f_{D_{\max,n}}$ within the corresponding signal block will be measured in an ambiguous way.

$$f_{D_{\text{meas,n}}} = f_D\,(\bmod f_{D_{\max,n}}) \quad (13)$$

Since the CRF within N consecutive transmit signal blocks is different, ambiguities can cause the measured Doppler

frequencies $f_{D_{\text{meas,n}}}$ to be different also, as depicted in Fig. 6, according to the applied CRF.

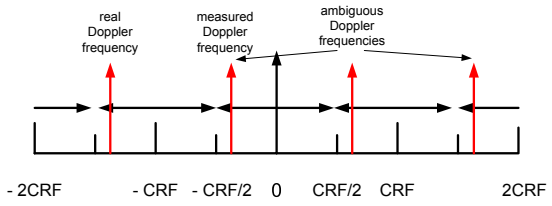

Fig. 6. Ambiguities in Doppler frequency masurement

Choosing the 2 or 3 adjacent transmit signal blocks with properly chosen chirp duration T_{chirp}, the unambiguous Doppler frequency f_D can be estimated and calculated from the different Doppler frequency measurements $f_{D_{\text{meas},n}}$, $n = 1, 2, 3$ inside a single transmit signal block using the algorithm described in [1].

As shown in Eqn. 8 the target range related frequency f_B depends on the chirp duration T_{chirp} also. In order to generate a constant beat frequency f_B from signal block to signal block, the system bandwidth has to be adapted accordingly. Keeping f_B constant reduces the complexity of the unambiguity resolution algorithm, since only a one dimensional search has to be carried out. Also, the spatial frequency, introduced by the target's azimuth position, is not influenced and will stay constant. Consequently, the ambiguity resolution algorithm can be applied to each antenna receive beam separately.

B. Ambiguity Resolution Algorithm

According to Fig. 7, the algorithm can be described by the following processing steps.

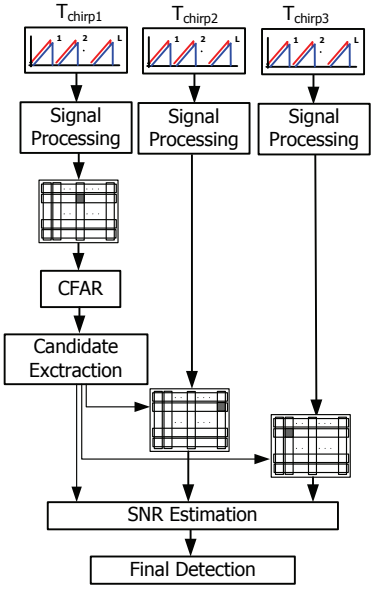

Fig. 7. Algorithm for resolution of ambiguous targets

1) Signal Preprocessing: Signal Processing in each transmit signal block is carried out according to section III.

2) Preliminary Target Detection: Usually, ambiguity resolution algorithms are applied to N lists of detected plots. This approach requires a detection procedure to be conducted in each signal block. The discussed algorithm on the other hand requires only a single detection procedure within the first signal block resulting in a single list of detected plots. After computing the spectrum for each beam in transmit signal block n, preliminary plots are generated by application of a two-dimensional CFAR algorithm to each beam. Since no detection is being carried out in the following $N-1$ signal blocks, probability of detection within block n has to be high. But since there is a downstream second threshold test, false plot detections are of little importance. This step can be understood as a data reduction step.

A first estimation of possibly ambiguous target parameters (R, v_r, φ) is done on basis of the spectral position $(\hat{u}, \hat{v}, \hat{w})$ of the peaks in $S(u, v, w)$.

3) Calculation of Candidate Plots: From the preliminary, possibly ambiguous plots (R, v_r, φ) detected in the spectrum of block n, candidate plots are calculated by adding a multiple of the maximum unambiguous velocity $v_{r_{\text{max,n}}}$ to the estimated radial velocity $v_{r_j} = v_r + j \cdot v_{r_{\text{max,n}}}$, $j \in [-J/2, J/2-1]$. The parameter J is defined by the maximum expected radial velocity.

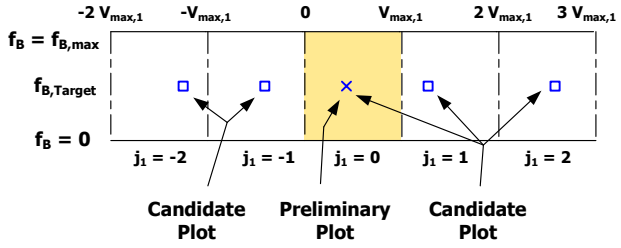

Fig. 8. Possible candidate plots

4) Signal and Noise Power Estimation: After generation, the candidate plots (R_j, v_{r_j}, φ) have to be evaluated. This is done by estimating the respective signal and noise power $\text{SNR}_{j,k}$ of a candidate plot within all blocks $k \in [n, n+N]$ and integrating all N estimates.

$$\text{SNR} = \max_j \left(\sum_{k=n}^{n+N} \text{SNR}_{j,k} \right) \tag{14}$$

For each detected plot, only the candidate plot with the highest combined SNR_j is propagated. Also, all single block $\text{SNR}_{j,k}$ of candidate plot j have to exceed an properly chosen threshold T_k.

5) Final Target Detection: In the final processing step, the estimated signal to noise ratio SNR of the best candidate plot is compared to a second threshold T.

$$\text{SNR} \geq T \tag{15}$$

At this point the final decision for plot j is made. A target is detected, if SNR exceeds the threshold T (Eqn. 14).

V. Simulation Results

In this section an simulation of the proposed radar system with exemplary parameters will be presented. The considered simulation setup is depicted in Fig. 9.

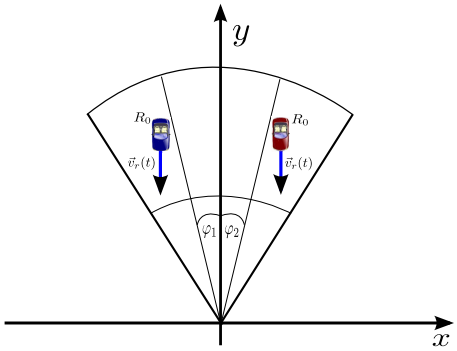

Fig. 9. Simulation setup

Both targets are placed at a range of $R_0 = 10\,\mathrm{km}$ and have a radial velocity of $v_r = 20\,\frac{\mathrm{m}}{\mathrm{s}}$, which is larger than the maximum unambiguous velocity range. The only difference between the two targets is their azimuth angle position. For the first target it is assumed to be $\varphi_1 = 10\,\mathrm{deg}$ and for the second $\varphi_2 = -10\,\mathrm{deg}$.

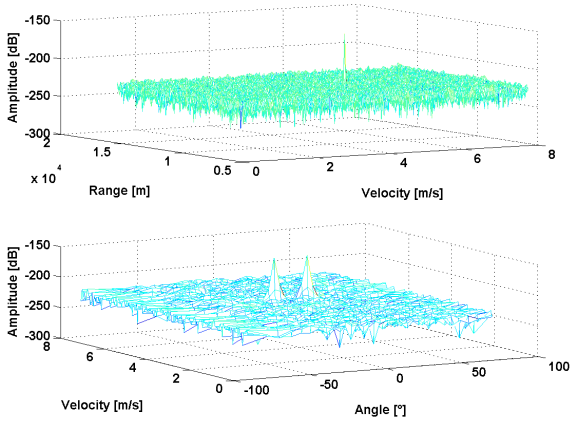

Fig. 10. Range-Velocity and Velocity-Angle plots using one signal block

The upper figure in Fig. 10 shows the situation in a two dimensional plot without azimuth angle resolution. Although two targets are present,only a single target has been detected. The lower figure depicts the measurement setup in a velocity-azimuth plot, clearly showing the separation in azimuth angle. It can be further noticed that the radial velocity, since it is greater than the maximum measurable radial velocity $v_{\max}$, is not estimated correctly.

Fig. 11 on the other hand shows the targets in a two dimensional velocity-azimuth plot, where three blocks with chirp durations of $T_{\text{chirp},1} = 25/26 \cdot T_{\text{chirp}}$, $T_{\text{chirp},2} = T_{\text{chirp}}$ and $T_{\text{chirp},3} = 27/26 \cdot T_{\text{chirp}}$ are depicted, where T_{chirp} is the chirp duration. It can be observed, that the peak has

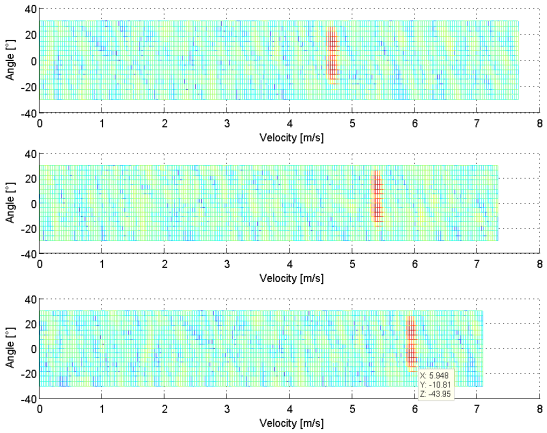

Fig. 11. Velocity-Angle plots using three signal blocks with different chirp durations

a similar beat frequency component, but a different radial velocity component v_r. According to the algorithm described described in section IV-B, the true radial velocity can be estimated to be $v_r = 20\,\frac{\mathrm{m}}{\mathrm{s}}$.

VI. Conclusion

This paper presents an FMCW waveform design introducing a linear receive antenna array as well as an algorithm for extending the unambiguous Doppler range and gives an explanatory target constellation. It has been shown, that the range of a target can be deduced from the beat frequency f_B due to the objects range and that the Doppler frequency can be estimated considering several modulation periods in a very precise manner. Furthermore, by means of a linear antenna array, the target azimuth angle can be estimated as well very precisely. Additionally, an algorithm has been presented, which is able to eliminate any ambiguities in Doppler frequency estimation considering consecutive signal blocks with different chirp durations T_{chirp}.

References

[1] H. Rohling, "Resolution of Range and Doppler Ambiguities in Pulse Radar Systems," in *Proceedings of Digital Signal Processing*, Flornce, 1987.

[2] A. L. Dzvonkovskaya and H. Rohling, "HF Radar Ship Detection and Tracking Using the WERA System," in *Proceedings of the International Conference on Radar Systems*, Edinburgh, United Kingdom, October 2007.

[3] H. Griffiths, "New Ideas in FM Radar," *Electronics & Communication Engineering Journal*, vol. 2, pp. 185–194, October 1990.

[4] A. Stove, "Linear FMCW Radar Techniques," *Radar and Signal Processing, IEE Proceedings F*, vol. 139, pp. 343–350, 1992.